UNIVERSITY OF GÄVLE

FACULTY OF ENGINEERING AND SUSTAINABLE DEVELOPMENT
Department of Building Engineering, Energy Systems and Sustainability Science

Testing of an innovative metal nanothread heat flux sensor

Hector Sanchez

2019

Student thesis, Advanced level (Master degree, two years), 30 HE
Energy Systems
Master Programme in Energy Systems

Supervisor: Janne Akander
Assistant supervisor: Magnus Mattsson
Examiner: Mathias Cehlin
Assistant examiner: Arman Ameen

Preface

This thesis would have not possible without the help and collaboration of *JonDeTech AB* thermal sensors company. They allowed us to have their sensors and helped in any matter they could when any doubt appeared on the way.

Next, I would like to thank Jan Akander, my supervisor, who with his constant guidance allowed me to carry on.

Finally and most important, to my girlfriend Clara, who kept insisting me to work and focus when I felt a bit lazy.

Many thanks.

Abstract

Thermal sensors are currently highly used in building applications to assess losses and determine possible thermal bridges. However, in some cases they are not useful enough because of the field conditions or, sometimes, due to the dimensions of the sensor.

This thesis aims to calibrate and test a new product developed by *JonDeTech AB* company; a tiny heat flux - temperature sensor based on metal nanothreads and a vertical or "out-of-the-plane" thread arrangement. It may have a bright future in measuring local heat flux through building and installation components owing to its tininess.

Three methods have been applied. First, calibration with a specific device designed for this purpose in a controlled environment. Second, field test measurements within an ongoing project by *Gävle* University in *Gävle* city hall historical building. And third, finite element simulations where the experimental scenarios were replicated. By these methods it was possible to apply corrections on the experimental procedures and make this work more accurate. It was also determined, the calibration curve of the sensor and a slight temperature dependency. In the field measurements, the output of the new heat flux sensor (using the calibration curves) was compared with output from a heat flux sensor available on the market. There is a good correspondence in the dynamics of the two sensors output, but there are discrepancies in the order of magnitude. Finite element simulations indicate that differences in the incidental direction of heat through the sensor are different in-situ and calibration, thus affecting results. Larger deviations are obtained for lower heat flux values (< 10 W/m2). These differences suggest that the calibration procedure can yet be improved.

Regarding the usefulness of the studied sensor, its tininess makes it a perfect measurement device in little spaces such as small cavities or narrow frames where other sensor cannot even be placed and also disturbs much less than the ones in the market. Nevertheless, it still can be further developed i.e. encapsulating it in a non-metal guard that would interfere less with the incidental heat.

Table of contents

1 Introduction

1.1 Background

Nowadays the Earth is undergoing a huge threat. Scientific evidence for warming of the climate system is unequivocal. Atmospheric CO_2 levels have been increasing over 50 years, the planet's average surface temperature has risen about 0.9 degrees Celsius since the late 19th century, Greenland and Antarctic ice sheets have decreased in mass, global sea level rose about 20 cm in the last century and a large etcetera that evidences the Earth's condition.

At sight of this menace, it is important for the humankind to reduce the CO_2 emissions and try to make our energy consumption as environmentally friendly as possible.

Therefore, energy efficient and nearly zero CO_2 emissions buildings are the main objective in present-day Northern countries. For this reason, many researchers are currently studying, among other fields, more effective insulation materials and structural building elements. To test the performance of these elements such as windows and doors it is usual to assess the performance of each component and the whole element.

With this purpose, hotboxes use is widely spread in order to measure important element properties like U-values, thermal losses and potential thermal bridges. However, when it comes to historical buildings they are not useful enough because of the fact that the façade elements cannot be modified and sometimes have poor thermal comfort inside them; moreover, the materials used in the construction are often unknown. Hence, it is needed a better approach than hotboxes, a device that is able to be easily carried and installed; heat flux sensors are the solution that deal with the exposed issue.

During the semester this thesis took place, there was an ongoing project in the *Gävle* city hall building, classified as historical, where researchers from the University of *Gävle* set up a system to assess thermal losses through the 18th century building windows. At the same time, *JonDeTech AB,* a relatively new technological company, ended the developing of their new product: a heat flux sensor based on metal nanothreads (similar to a thermopile sensor but smaller in size, a tiny cylinder of 10⌀ x 1.6 mm).

In order to achieve accurate measurements, this new sensor needs calibration and field testing. Since its dimensions are tiny, it is ideal for assessing heat losses through small building components, such as window wooden frames. The idea of using the device in the city hall project was realized since possibility of comparing performance of this sensor with heat flux sensors (*Hukseflux*), available on the market and used in the project. Hukseflux has the dimensions 80 x 6 mm.

1.2 Literature review

There has been important improvements in the research area of thermopiles and historical buildings assessments in the course of the past two decades.

From the common foundation of the thermopiles, tremendous development has been made in thermopile based systems, in such areas as fabrication, sensitivity, versatility, size and sensing directions. A study in 2004 found increased sensitive thermopiles with different metals and combinations [1]. In the chemistry field it was possible to create a calorimeter to measure enzyme catalysed reactions through a continuous flowing fluid with very low detection limits (a few [mW/l] of precision) [2].

Regarding the miniaturization of the sensors, in 2008 a calorimeter was developed by researchers from China, using a microelectromechanical system. It was built as a 2D flow sensor with an etched structure containing a fine membrane that senses temperature difference in both directions (with an angle error of 3°). With this device it was possible to determine thermodynamic properties of particles as small as biomolecules [3]. Another example comes from Germany: it was possible to miniaturise a thermal flow sensor by using a high-temperature thermopile fabrication process, making it also suitable for other applications [4].

The sensor tested in this thesis is able to function as an infrared (IR) sensor besides as a thermopile. One possible application will be to install it on mobile devices such as cell phones, it is important then to take a look at the work done by the Finnish researchers: as they confirmed, the current IR systems in mobile devices can produce inaccurate readings. They were designed for the device being in steady state and for measuring temperatures warmer than the device itself, often these assumptions are not fulfilled causing an error of several degrees. Therefore they designed and calibrated a new optomechanical structure that solved the previous conditions [5].

Later on, in 2011, researchers from Louisiana, USA, developed some thermopile designs where they changed the junction of the metal threads that connect the sensing parts. With these improvements the thermopile was either blind or sensitive to different thermal flows such as axisymmetric, linear or non-linear; depending on the orientation [6].

On the other hand, there are specific studies on the field of building constructions and engineering, from experimental hot boxes used to assess losses to developed software applications to simulate thermal conditions and estimate losses and efficiency.

For instance, EPICAC-BE is a dynamic energy simulation software designed by the Budapest University using MATLAB. It was used to study the window's refurbishment of Central-European historical building. Results showed that the use of double glass windows is not always the best option looking at the overall efficiency [7]. From Ireland, a lot of materials have been tested and compared against the manufacturer's properties in order to improve the wall insulation of historical buildings [8]. Also in the United Kingdom, same kind of study has taken place inside the solid walls of a typical Victorian house - results show again that field measurement results tend to be worse than the ones done in a testing facility [9].

Regarding the hot boxes applications, there are several examples that show the progress of this research field. Back in 1984, the University of California noted that to assess the window performance it was not enough measuring its energy losses in situ. Instead, it was necessary

to design a unique testing facility (the MoWiTT), becoming one of the first precedents for modern hot boxes [10].

In 2017, the University of Perugia, Italy, proposed an experimental assessment for dynamic thermal properties of building parts. Inside a hot box and using heat flow sensors and infrared thermography they were able to determine the correct properties of the studied components [11]. In an additional research, they tested, characterised mechanically and assessed the thermal conductivity of some mortar samples using a specific apparatus called 'small hot-box' which was meant for this idea; comparing the results with a heat flux sensor they were reliable and quite accurate [12]. Another example comes from the University of the Basque Country as an analysis of thermal bridges inside a hot box set up and physics simulation in parallel [13]. Still in the area of thermal bridges, investigators from Portugal studied the thermal behaviour of a wooden structured building; specifically of a corner pointing to the outside. They found out that even with an extra insulation layer on the corner, more heat was being lost through the thermal bridge created by the wood in the corner than through the walls without any insulation [14].

Some other studies even advice on how to calibrate hot boxes by using different temperature control strategies e.g. the investigation done by Indian researchers where they proposed three different approaches, all giving great results within the standards [15]. However, when comparing the standards, researchers from Italy found out that the European EN ISO 8990 and the American ASTM C1363-05 seem to need an improvement that the Russian GOST 26602.1-99 already has: when testing heterogeneous parts, each component of the part should be measured individually [16]. The European and American standards measure only the total heat passing through entire constructions (thermal bridges included in the U-value) while the Russian standard distinguishes U-values of individual components in the measurement, thus giving more information and more exact U-values of the monitored system.

It is also worth of mention articles that focus on making glazing with switchable U-values for better adaptation to different climate i.e. one for winter months (more solar radiation is allowed inside the building) and one for summer months (less solar radiation goes inside) [17]. And new models created in order to study these modern glazing units [18][19].

In conclusion, it is usual to do experimental tests on building components in a laboratory environment. Hot boxes are often used with this purpose and there are also standards for the creation and calibration of them. Moreover, as stated in [16], the use of hotboxes together with heat flow sensors will give the most informative and accurate results (such as U-values) for more complex tested systems, such as windows. Though testing and validation of thermal performance of systems/components, the review indicates that these behave worse when exposed to their natural environments than in laboratories. In field measurements, it is necessary that sensors are calibrated and, the components seem to behave a bit worse when taking the studies to the field. It is important then to make sure that the used sensors are calibrated and accurate enough. Hence, each type of thermal device needs its own calibration; from the literature review it is found that each type needs its own calibration set

up. So, in this work a unique calibration set up will be designed for the *JonDeTech* thermopile sensor. Moreover, the *JonDeTech* sensor will be tested in field conditions.

It is common as well to confirm the measurement with computer simulations. Therefore, the calibration system and the field measurements will be replicated in *Comsol Multiphysics* (CM), a finite element simulation program that allows to couple different physics, here specifically thermal steady-state and air flow dynamics.

It is significant to emphasise the importance of studying thermal bridges in buildings, so that they can be easily found and properly insulated when the building process is ongoing. This can be classified as one of the main objectives of an excellent thermal insulated building. However, thermal bridges appear wherever heterogeneous components meet. The tininess of *JonDeTech* new sensor could be useful in this aspect since it allows to make measurements in small regions where it is known to exist a thermal bridge e.g. the window frames typical from historical buildings.

1.3 Aim

The main objective of the current thesis is the test of *JonDeTech* new heat flux sensor in the laboratory facilities and in field measurements too. That is, determining the calibration curve, or curves, that relate voltage [μV] and heat flux [W/m^2] taking into account any temperature dependence. And to test if *JonDeTech* performance, based on calibration data, in field measurements are comparable to that of a heat flux sensor that is already available on the market, *Hukseflux HFP01*.

As a sub-objective: to build a calibration apparatus that will be able to be used to calibrate other sensors available on the market, as well as the studied one. In this way, the calibration set-up and apparatus will be validated.

1.4 Approach

In order to complete the aim three approaches will take place:

- Laboratory tests and calibration: by controlling temperatures inside a climate chamber it will be possible to determine the calibration significant parameters.
- Field measurements: at least one in *Gävle* city hall and another one in *Gävle Energi* fluid pipes if possible.
- Computational finite element simulation: to identify how heat is flowing through all the elements of study and allow corrections if needed.

2 Theory

2.1 Thermocouples

A thermocouple is an analogical sensor that transforms a temperature signal into a proportional voltage signal. Thermocouples are made by the junction of two different metal wires connected on one sensing end. Their main use is widely spread as a temperature sensor.

Thermocouples are usually used in industry and scientific applications, some of them include temperature measurement for kilns, thermostats, safety devices, gas turbine exhaust, diesel engines, and other industrial processes.

Thermocouples are self-powered and require no external form of energy whereas most other methods of temperature measurement do. They are based on Seebeck effect. [21]

2.2 The Seebeck effect

In 1821 Thomas Johann Seebeck observed that a compass needle was deflected when a temperature difference was applied between the ends of two different metals joined by a closed loop. He recognized that the electron energy levels in both metals moved dissimilarly, therefore, a potential difference appeared creating a current and a magnetic field around the wires [21].

$$J = \sigma \cdot (-\nabla V + E_{emf}) \qquad \textbf{(1)}$$

The physics behind the Seebeck effect can be described by the equation 1. Where **J** is the current density [A/m^2], $\boldsymbol{\sigma}$ represents the electrical conductivity [S/m], $\boldsymbol{\nabla V}$ is the voltage gradient [V] and $\mathbf{E_{emf}}$ is the electromotive force [V].

When steady state is reached **J** becomes zero and expressing the electromotive force in terms of local temperature; it is possible to write the directly proportional relation between voltage and temperature difference as showed in equation 2.

$$0 = \sigma \cdot (-\nabla V - S \cdot \nabla \mathrm{T}) \qquad \text{then} \qquad -\Delta V = S \cdot \Delta T \qquad \textbf{(2)}$$

Where **S** represents the Seebeck coefficient [V/K] (usually [μV/K]), used in thermocouples devices, it changes depending on the type of metals.

2.3 Thermocouples types

In Table 2. 1 the different thermocouple types are summarised. In this thesis T-type thermocouples have been used in the experimental procedures.

TABLE 2. 1. THERMOCOUPLE PROPERTIES SUMMARY [22]

Type	Composition	Temperature range	Seebeck coefficient [μV/K]
E	Chromel - Constantan	-110 to 140 ºC	68
J	Iron - Constantan	-40 to 750 ºC	55
K	Chromel - Alumel	−200 to 1350 ºC	41
M	Nickel – Molybdenum - Cobalt	0 to 1400 ºC	-
N	Nicrosil – Nisil	-270 to 1300 ºC	39
T	Copper - Constantan	-200 to 350 ºC	43
B	Platinum – Rhodium	50 to 1800 ºC	10
R, S	Platinum – Rhodium	0 to 1600 ºC	10
C, D, G	Tungsten – rhenium	0 to 2329 ºC	20

2.4 Thermopiles

By connecting several thermocouples in series, or less often in parallel, a thermopile device is made. It also generates electrical energy by transforming thermal energy.

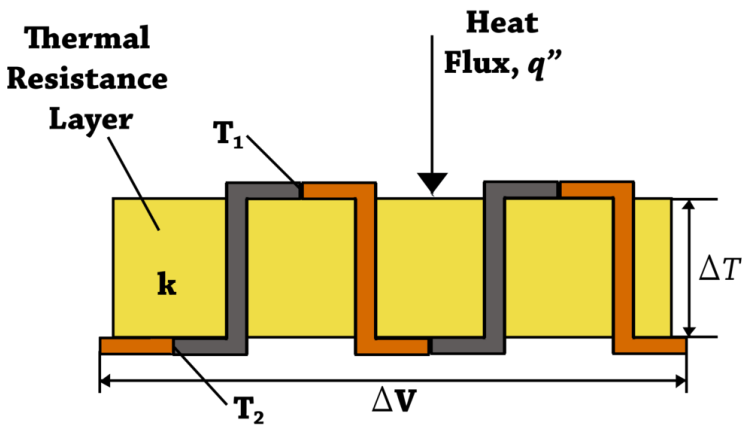

FIGURE 2. 1. DIAGRAM OF A THERMOPILE WITH TWO SETS OF THERMOCOUPLES ARRANGED IN SERIES (GREY AND ORANGE). IN BETWEEN THERE IS A THERMAL RESISTANCE LAYER (K).

In Figure 2. 1, a thermopile diagram is shown. The top side junctions are at T_1 while the bottom side ones are at T_2. The created output voltage is proportional to the temperature difference $\Delta T = T_1 - T_2$ and to the incidental heat flux as well which is function of the metal junctions, too.

Thermopiles are widely used in heat flux sensors and many other applications such as pyrheliometers (sensor to measure direct solar beam irradiance), infrared thermometer, thermal accelerometers and gas burner safety controls. They can be also used to generate electrical energy using the thermal energy from: heated electrical components, solar wind, radioactive materials, laser radiation or combustion [24].

The output from the heat flux sensor is the voltage created by the temperature difference over the sensor. In order to convert this entity to heat flux [W/m^2], the device needs to be calibrated.

A robust sensor will have a linear performance, according to equation 2. By having a calibration assembly, measurement of the output voltage from the sensor and knowledge about how much heat passes through it, will give the constant (or curve, if dependent on for example temperature of the sensor).

2.5 *JonDeTech AB* thermopile sensor

Thermopile threads can be arranged in various ways, nowadays is typically used the horizontal or "in the plane" architecture. This structure is caused by the process of fabrication which historically was developed to make lateral assemblies on silicon, in the same plane. However, it seems not to be the best solution since cold and hot junctions are placed next to each other on the same surface, in terms of Figure 2. 1, T_1 and T_2 temperatures will be located on the same plane. Therefore thermal interferences may cause wrong measurements.

JonDeTech AB used a vertical thermocouple thread arrangement similar to Figure 2. 1. Hence, hot and cold junctions are isolated one to another by the thickness of the substrate. Then, the heat gradient is through the substrate. This vertical configuration requires that the leads of the thermocouples are created through the substrate material, creating tiny holes tightened to the threads. Thermocouple lead-structures based on nanotechnology had been realized, which is what *JonDeTech AB* offers [24].

In Figure 2. 2 it is shown the current structure of this sensor. The thermopile sensing part is located in the middle of the top drawing in dark grey, it is encapsulated by brass metal plates, the connections are made of silicon and the board where the electric circuits are printed is made of kapton.

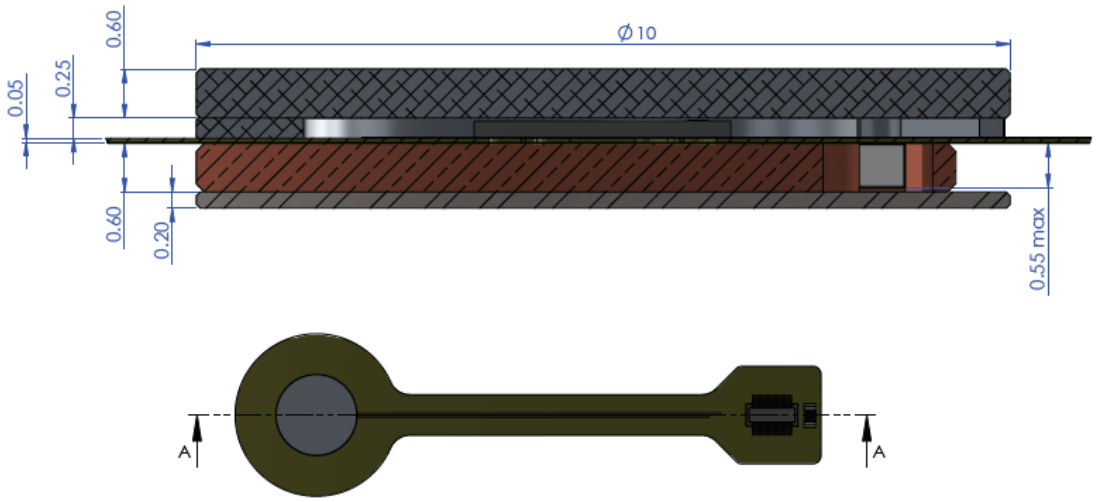

FIGURE 2. 2. BOTTOM, WHOLE SENSOR WITHOUT THE CONNECTING WIRE: GREY PART IS DETAILED ON TOP AND GREENISH PART IS THE KAPTON TAPE CONTAINING THE SILICON CIRCUITS. TOP, DETAIL OF THE SENSING PART AND ITS BRASS GUARD, MEASURES ARE SHOWN IN [MM].

It could be problematic that the capsule is made of a good heat conductor such as brass, because of the fact that the incidental heat flux may escape the kapton sensing part. That is one crucial point on the work.

2.6 Heat flux in water pipes

In order to study the heat flux that is being lost on a water pipe. The equations that will be used are presented and explained on this item. It is shown the calculation of the heat supplied by the pipe and the approximation of the heat transfer convective coefficient, using Reynolds, Prandtl and Nusset numbers.

In Figure 2. 3 the nomenclature for the pipe is shown.

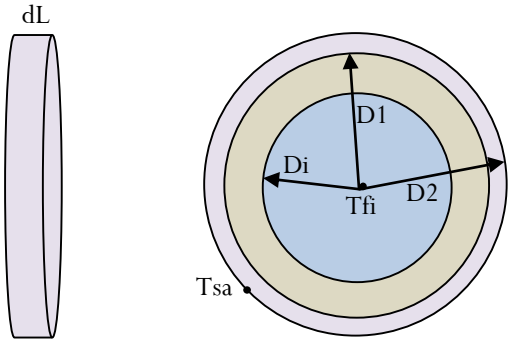

FIGURE 2. 3. A METAL PIPE RECOVERED BY INSULATION FOAM AND WATER FLOWING INSIDE. DI IS THE INTERIOR DIAMETER, D1 THE PIPE EXTERNAL DIAMETER, TFI IS THE TEMPERATURE OF FLOWING FLUID AND TSA REPRESENTS THE TEMPERATURE OF THE FOAM OUTER SURFACE.

Assuming a differential of longitude in a pipe, the heat flux coming out of the pipe is shown at equation 3: where **q** is the heat flux, **A** is the area and $\boldsymbol{\phi}$ is the heat.

$$q = \frac{\phi}{A} \quad \frac{[W]}{[m^2]} \tag{3}$$

The Area expressed in terms of longitude differential is shown at equation 4.

$$A = \pi D_2 dL \tag{4}$$

If equations 3 and 4 are combined and developed using the thermal resistances through the pipe layer it is possible to get equation 5.

$$q = \frac{\phi}{\pi D_2 dL} = \frac{(T_{fi} - T_{sa})dL}{\left[\frac{\pi D_2}{\pi D_i h_1} + \frac{\pi D_2}{2\pi\lambda_1} ln\left(\frac{D_1}{D_i}\right) + \frac{\pi D_2}{2\pi\lambda_2} ln\left(\frac{D_2}{D_1}\right)\right] dL} \tag{5}$$

$$q\left[\frac{\pi D_2}{\pi D_1 h_1} + \frac{\pi D_2}{2\pi\lambda_1} ln\left(\frac{D_2}{D_i}\right) + \frac{\pi D_2}{2\pi\lambda_2} ln\left(\frac{D_2}{D_1}\right)\right] = (T_{fi} - T_{sa})$$

In equation 5 $\boldsymbol{\lambda_i}$ represents the heat conductivity of the solid parts and $\mathbf{h_1}$ is the convection coefficient of the flowing fluid, which is depends of the type of liquid, the velocity and the

pipe. It is function dependant of Reynolds, Prandtl and Nusselt numbers. If the thermal resistance of all layers is merged in one equivalent resistance it can be written as equation 6.

$$T_{fi} = T_{sa} + R_{eq} q \pi D_2 \quad \textbf{(6)}$$

Then, Reynolds number calculation is shown at equation 7, where $\boldsymbol{\rho}$ is fluid density, **u** is the relative velocity as seen from the pipe, **L** is a characteristic linear dimension (internal diameter for circular pipes), $\boldsymbol{\mu}$ is the dynamic viscosity otherwise $\boldsymbol{v}$ the kinematic viscosity can be used.

$$Re = \frac{\rho u L}{\mu} = \frac{u L}{v} \quad \textbf{(7)}$$

Prandtl number, at equation 8, where $\boldsymbol{\alpha}$ is the thermal diffusivity, $\mathbf{c_p}$ is the specific heat and **k** represents the thermal conductivity.

$$Pr = \frac{v}{\alpha} = \frac{c_p \mu}{k} \quad \textbf{(8)}$$

After calculating Re and Pr, Nusselt number can be approximated by Dittus-Boelter correlation in equation 9, where **n** can be 0.3 for a cooling fluid or 0.4 for a heating one.

$$Nu = 0.023 Re^{0.8} Pr^n \quad \textbf{(9)}$$

Finally, the convective heat transfer coefficient **h** can be estimated with equation 10 [25].

$$Nu = \frac{hL}{k} \qquad h = \frac{Nu \cdot k}{L} \quad \textbf{(10)}$$

3 Method

On the next item the used method for the elaboration of this thesis is explained.

Firstly, it was simulated on finite element software the experimental scenario. After that, some corrections took place in the experimental system design, so the measurements and data acquisition could be more accurate. The sensor was calibrated inside a climate chamber while controlling the boundary conditions. Next, it was tested in field measurements and, finally, the obtained results were analysed statistically.

3.1 Laboratory work

In this topic, the work taken place in a controlled environment is explained, inside *Gävle* University laboratory facilities.

It was necessary to design a device that allowed the calibration of the sensor. With that in mind, it was needed to know accurately the supplied heat and ensure that it went through the sensor perpendicularly and in a uniform manner as showed in Figure 3. 1; so that the measured thermal flow had no effect because of the angle of incidence. It also had to allow an efficient cooling towards the environment, due to this reason aluminium fins were added to ease the convection towards the climate chamber. It is also necessary that the whole set-up is at steady-state, i.e. that heat flows and temperatures are constant in time. This criteria will assert that the amount of heat that is supplied to the system is equal to the amount of heat that is transmitted from the system.

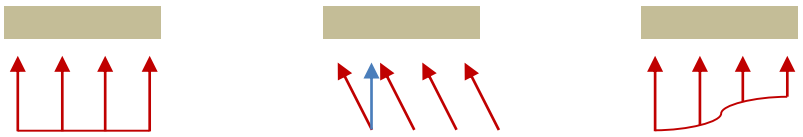

FIGURE 3. 1. EFFECT OF THE HEAT FLUX GOING THROUGH THE SENSOR. LEFT FIGURE REPRESENTS THE DESIRED SCENARIO, A UNIFORM NORMAL HEAT FLUX. MIDDLE FIGURE SHOWS A UNIFORM FLUX WITH CERTAIN ANGLE OF INCIDENCE, THE BLUE LINE REPRESENTS THE HEAT FLUX MEASURED BY THE SENSOR AND THE RED ONE THE SUPPLIED. RIGHT FIGURE SHOWS A NORMAL AND NOT UNIFORM FLUX.

To sum up, next points where needed in the calibration device:

- A heating power supply with control
- Insulation to ensure that heat is going towards the sensor
- Uniform perpendicular heat flow
- Efficient cooling
- Minimise unintentional losses to the environment

At first it was thought to be used symmetry because two of the studied sensors were available. By placing one heater between two sensors it can be easily calculated the heat flux flowing in them, which is half of the supplied one. However, a heater as small as the studied sensor was not available.

Therefore, another option was necessary: the proposed solution to fulfil these points is displayed at Figure 3. 2. It shows a device covered by insulating foam (Kingspan foam) to reduce losses to the environment.

At the bottom of the device there are 2 heaters attached over a FR4 circuit board. They are controlled each one by a different PID control system. In order to get the whole input heat from the top heater going upwards, the bottom heater is adjusted to maintain the same temperature as the top one; by reaching this scenario in steady state, an adiabatic condition appears between the two heaters because of symmetry. Each heater has an inner (on the circle but not on the circumference) and an outer (around the circumference edge) heating part which can be regulated individually.

Following the assembly upwards, a thicker copper plate was placed so that the heat flux could spread out uniformly. That was possible by using a really high thermal conductive material, in this case copper plates that were available in the laboratory.

Next, it was necessary to have the sampling of the temperatures above and below of the sensor. Therefore, thermocouples were installed. So, in order to avoid air cavities around the wires that would interfere with the desired heat transfer by adding convection and long wave radiation to the system, a conductive flexible plastic film was used. Between two thin sticky layers of the plastic three thermocouples were placed (centre, edge and middle, Figure 3. 3a). This plastic not only provided a layer to avoid cavities next to thermocouples but also helped to keep the contiguous layers more attached to each other by improving the contact with its stickiness.

After the plastic film, the sensor itself was located, it was encompassed by a brass ring with a similar thermal conductivity in order to keep this layer's uniformity. Its assembly is shown in Figure 3. 3b.

Next, another conductive plastic film with thermocouples and another copper plate to spread out the heat all around the device were installed, too.

Finally, eight trapezoidal aluminium fins including their thin aluminium base were installed to ease the cooling convection with the air. Detailed drawings for the whole assembly are displayed in Appendix A.

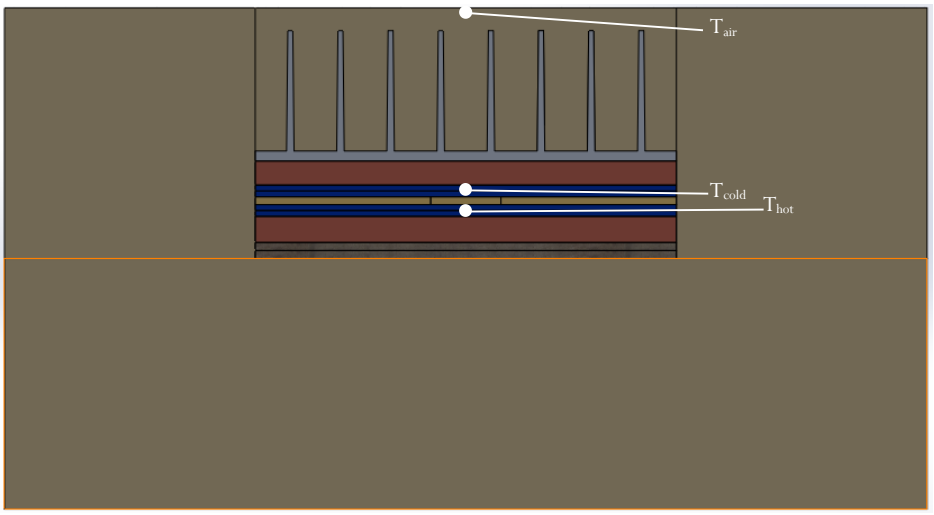

FIGURE 3. 2. MIDDLE CROSS SECTION OF THE CALIBRATION DEVICE USED IN THE LAB. FROM BOTTOM TO TOP: INSULATING FOAM, SECONDARY HEATER, PRIMARY HEATER, COPPER PLATE, CONDUCTIVE FILM WITH THERMOCOUPLES, BRASS AND SENSOR, CONDUCTIVE FILM WITH THERMOCOUPLES, COPPER PLATE AND ALUMINIUM FINS.

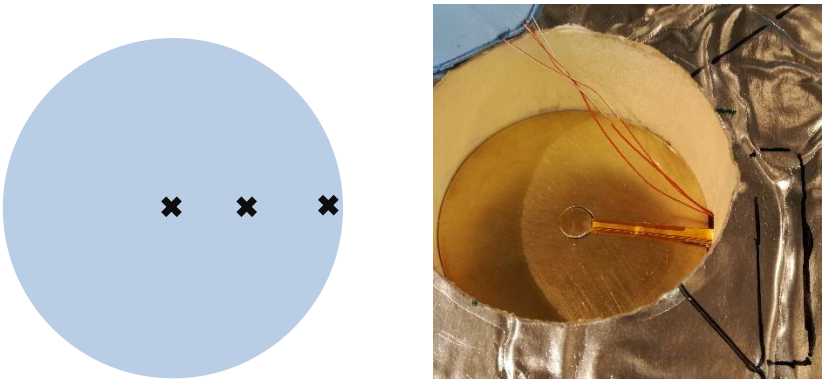

a b

FIGURE 3. 3. A: THERMOCOUPLE LOCATION WITHIN THE CONDUCTIVE FILM AS SEEN IN TOP VIEW. B: BRASS RING AND TESTED SENSOR ASSEMBLY.

It was also necessary to open a hole in the insulating foam in order to allow a path for the wires and the sensor itself. A piece of insulation was cut at the sensor height, through that hole it was possible to pass all the required wiring. After that, the insulation piece was placed again on the assembly to keep with the insulating even though it was previously removed, it was simulated as well to check the effect of the temporary fix. Moreover, all the set up was compacted by a jig and some weight over all the structure to avoid any cavities between layers as showed in Figure 3. 4.

FIGURE 3. 4. WHOLE ASSEMBLY OF THE CALIBRATION SYSTEM WITH THE JIG INSIDE THE CLIMATE CHAMBER.

Using this device and varying the temperature conditions (on the primary heater and on the climate chamber's air) as well as some corrections coming from the simulations, it was possible to get a calibration curve for the sensor. Table 3. 1 shows the temperature values fixed on each experiment.

TABLE 3. 1. TEMPERATURE VALUES FOR THE EXPERIMENTS TAKEN PLACE IN THE LABORATORY

ID	Heater temperature [ºC]	Air temperature [ºC]
1	3	0
2	7	0
3	10	0
4	23	20
5	27	20
6	30	20
7	43	40
8	47	40
9	50	40
10	63	60
11	67	60
12	70	60

In order to determine the input heat, the supply voltage was measured for the primary and secondary heaters and the flowing current. Equation 11 shows the calculation done for each experiment to get the heat, where $\boldsymbol{\phi}$ is the supplied heat, $\mathbf{V_i}$ is the voltage on the inner primary heater, $\mathbf{V_o}$ represents the voltage on the outer primary heater, $\mathbf{I_i}$ is the current flowing through the inner primary heater and $\mathbf{I_o}$ is the current flowing through the outer primary heater.

$$\phi = V_i \cdot I_i + V_o \cdot I_o \qquad \textbf{(11)}$$

By dividing through the area (**A**) of the heater, which is the same as the hole on the calibration assembly, it is possible to determine the heat flux (**q**) as equation 12 shows below.

$$q = \frac{\phi}{A} \qquad \textbf{(12)}$$

It is important to emphasise the key aspect of steady state scenario, the first part of the experimental work was based on steady state. The variables that define the behaviour of the system, in this case temperature and heat flow, are unchanging over time. In continuous time that is, that the partial derivative of the significant variable with respect to the time is zero and remains as zero over time.

When steady state is reached and accordingly to the first law of thermodynamics all the supplied heat to the system equals to the leaving heat from the system since there is no work in it, equation 13 shows this condition. This is applied either for the whole calibration assembly either for only the studied sensor.

$$\Delta U = \phi - W \qquad \text{as } W=\Delta U=0, \text{ then} \qquad \phi_{supplied} = \phi_{leaving} \qquad \textbf{(13)}$$

Finally, on Table 3. 2 it is shown the thermal properties for the used materials, these values have also been used on the finite element computer simulations.

TABLE 3. 2. THERMAL PROPERTIES OF THE MATERIALS USED IN THE CALIBRATION DEVICE.

Material	Density [kg/m³]	Thermal conductivity [W/(m·K)]	Heat capacity [J/(kg·K)]
Kingspan foam	30	0.022	1400
Heaters board	1900	0.3	1370
Copper	8960	400	385
Conductive film	3.2	3	1
Brass	8553	109	380
Kapton (sensor parts)	1420	0.12	1090
Aluminium fins	2700	240	900

3.2 Computer simulations

The finite element method (FEM) is a numerical method for solving problems of engineering and mathematical physics. Typical problem areas of interest include structural analysis, heat transfer, fluid flow, mass transport, and electromagnetic potential. The analytical solution of these problems generally require the solution to boundary value problems for partial differential equations. The finite element method formulation of the problem results in a system of algebraic equations. The method approximates the unknown function over the domain. To solve the problem, it subdivides a large system into smaller, simpler parts that are called finite elements. The simple equations that model these finite elements are then assembled into a larger system of equations that models the entire problem. FEM then uses variation methods from the calculus of variations to approximate a solution by minimizing an associated error function.

Comsol Multiphysics is a cross-platform that applies finite element analysis, solver and multi-physics simulation software. It allows conventional physics-based user interfaces and coupled systems of partial differential equations. COMSOL provides a unified workflow for electrical, mechanical, fluid, acoustics, heat transfer and chemical applications.

Using Comsol Multiphysics software, three different scenarios were simulated that took place in the different parts of the method; laboratory work and field measurements (Figure 3. 5). The materials simulated were selected to be as close as the real ones, according to that, the properties used for the simulation are gathered together in Table 3. 2

3.2.1 Simplified version of the sensor

First, it was noticed that simulating the sensor in detail (that is with every small piece) the computational time to solve the FEM reached up to 5 hours. In order to reduce this enormous time a simplified version was modified and tested to make it as close as the real one. So, instead of making all the sensor pieces, they were replaced by a big solid one that cover up the sensor. With that, a lot of contacts between pieces were removed and replaced by simple heat transfer over one solid which theoretically will speed up the computation time quite a lot.

The boundary conditions applied were: a fixed temperature on the cold side of the surface at 0ºC and a warm convection condition on the other side and all the visible sensor parts; with a heat transfer coefficient of 12 $W/(m^2 \cdot K)$ and a warm indoors temperature of 20ºC.

This study used the predefined settings of Comsol Multiphysics in heat transfer in solids, steady state study and 3D geometry.

3.2.2 Calibration assembly

Secondly, the whole calibration assembly built in the laboratory part was simulated as well. Each material layer showed in Figure 3. 2 was added with the thermal properties expressed on Table 3. 2. Also, specific details were added in order to know its effect on the laboratory work: Those were:

- It was necessary to open a hole in the insulating foam to allow the access of wires. A similar hole was added in the simulation to check if its effect was significant enough to cause wrong measurements.
- The studied sensor had a kapton board attached to the thermopile itself, printed on the board there were the necessary electronic elements to transform and process the voltage analogical variable, such as amplifier, controller and analog to digital converter. The kapton board was also included on the simulation.
- A unique thermocouple was also simulated by placing two metal wires from the centre of the assembly to the external insulating foam at the height of the conductive plastic film. With that it was meant to study the effect of adding wires that conduct heat in the middle of the assembly. Probably the heating is conducted out of the insulation by the thermal bridge that the wires create.

The boundary conditions that were applied in this simulation were: a fixed power of 2W on the primary heater, which equals to $234 \cdot 10^3$ W/m^3 on the whole volume of the heater. Also, a fixed temperature on the surface between the two heaters according to the temperature reached when only the primary one is on after some iterations of trial it was defined as 28ºC. And a convection condition on the external surfaces with a heat transfer coefficient of 10 $W/(m^2 \cdot K)$ and an external temperature of 20ºC.

This second simulation used the same predefined settings of Comsol Multiphysics as the previous one: heat transfer in solids, steady state study and 3D geometry.

3.2.3 Sensor under the influence of convection

Finally, the last simulated scenario in Comsol Multiphysics was a field measurement that took place on the city hall window glazing. They simulated *JonDeTech* and *Hukseflux* sensors, the solution was used to compare and detect significant differences between brands on the convective boundary condition. Each sensor was placed on a glass surface with one cold side at a fixed temperature of 0ºC and one warm side affected by an indoor warm air flow. The air was considered as laminar on the study because it was flowing close enough to the glazing and with an average circulating velocity of 0.2 m/s [26].

The objective for this experiment was to detect different situations on the flowing air near the sensors and near the glazing surface. Since it was a hypothetical trial, the gravitational equations have not been included in the simulations. So, the effect of the buoyancy is not taken into account.

Last case of study used, fluid mechanics (specifically laminar flow) and heat transfer in solids physics that were coupled with the predefined settings of non-isothermal flow. It was a steady state study and used a 3D geometry. The main purpose was to investigate influence of convection on non-uniform heat conduction primarily in the *JonDeTech* sensor.

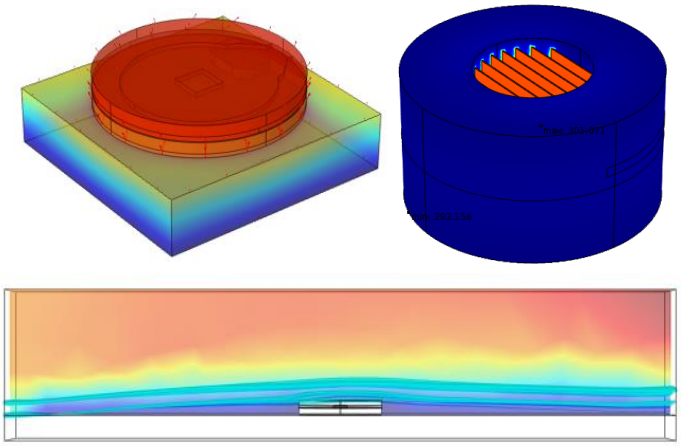

FIGURE 3. 5. CAPTURES OF THE SIMULATIONS SET WITH COMSOL MULTIPHYSICS SOFTWARE. UP LEFT: THE SENSOR WITH EACH PART RESTING ON A SURFACE. UP RIGHT: THE CALIBRATION SET UP USED ON THE WHOLE LAB WORK. BOTTOM: THE SENSOR ON RESTING ON A WINDOW GLAZING, THE AIR FLOW INLET ENTERS THROUGH THE LEFT SIDE.

3.3 Field measurements

3.3.1 *Gävle* city hall

Gävle city hall is located in the very centre of *Gävle* with address *Rådhustorget* 1. It was built between the years 1784 – 1790, on King *Gustav* III's assignment following drawings by architect *Carl Fredrik Adelcrantz* after the old one was burnt down in the city fire of 1776. The new one was designed in a French-inspired style with features of both rococo and classicism.

Gävle city hall building is classified as historical building. This condition does not allow to make any noteworthy changes on the façade that would destroy the harmony of the edification. As said in point 1.1, a project in the building was ongoing. Its main objectives were to assess thermal losses through the 18th century windows of the historical building and test new adhesive films that cover the windows glazing reducing the heat transfer on the glass without disturbing any of the façade elements.

The assembly consisted in building a hotbox within the window's niche by insulating one of the window's wall hole with foam, and inside replicate the indoors temperature and natural convection conditions.

Heating plates attached to the insulating foam surface facing the window where used to maintain temperature at 22 ºC and three heating rods placed on the window lintel were used to heat the bottom air and yield natural convection near the glazing, all the set up was controlled by a PID regulator. Thermocouples and heat flux sensors were used in order to get data from the experimentation. However, not everything could be monitored: some parts of the foam were cut in diagonal, window wooden frames were too narrow to place a heat flux sensor, etc.

Another problem appeared in sunny days, when too much solar irradiance was received, the insulated box reached temperatures over 50 ºC; even causing some sensors to unstick.

As a part of this project, the *JonDeTech* sensor was tested on the window frames, the insulation foam and the glazing.

3.3.2 Field measurements

The third crucial point of this thesis consist in taking the sensor on field measurement testing.

First, it was tested in the *Gävle* city hall historical building on some elements of the 18th century windows, they are shown in Figure 3. 6.

- Window glazing: it was placed next to a *Huksefkux* flux sensor in order to compare both of their readings, at the same height to avoid gradient temperature over the Z axis caused by natural convection. It was taped under the same conditions as the other sensor to minimise the unconsidered differences, that is, with toothpaste to improve the contact with the glass (this was a recommendation from *Hukseflux* manufacturers) and with sticky tape over it to keep its position fixed. The acquisition data period lasted for 24 hours.
- Wooden frame: it was tested on the lateral frame and on the central thicker frame. Here, it was placed at the same height as other thermocouples in order to use the temperature and the heat flux measurements to determine the thermal conductivity of the timber. It was also placed with sticky tape and toothpaste to maintain the position and to improve the surface contact. The acquisition data period lasted for 40 minutes for each analysed frame.
- Insulation foam: the insulation had to be cut in a diagonal manner so that it could fit in the window's niche, as it is shown in Figure 3. 6a top right picture. In order to determine differences between this cut and the ordinary insulation and also the proper thermal isolation, the sensor was placed there. It was also placed using toothpaste on the contact surface with the foam and covered with opaque sticky tape to prevent it from moving. The acquisition data period lasted for 24 hours.

All the field measurements took place on cloudy days or at night, so that the sun irradiance did not interfere or disturb the sensor's measurements, due to sun direct radiation that would have heated the entire system too much.

Those particular locations were selected because no other heat flux sensor used in *Gävle* city hall project could fit on them. Except for the glazing, when it was placed there, it was possible to compare its readings against *Hukseflux* commercial sensor.

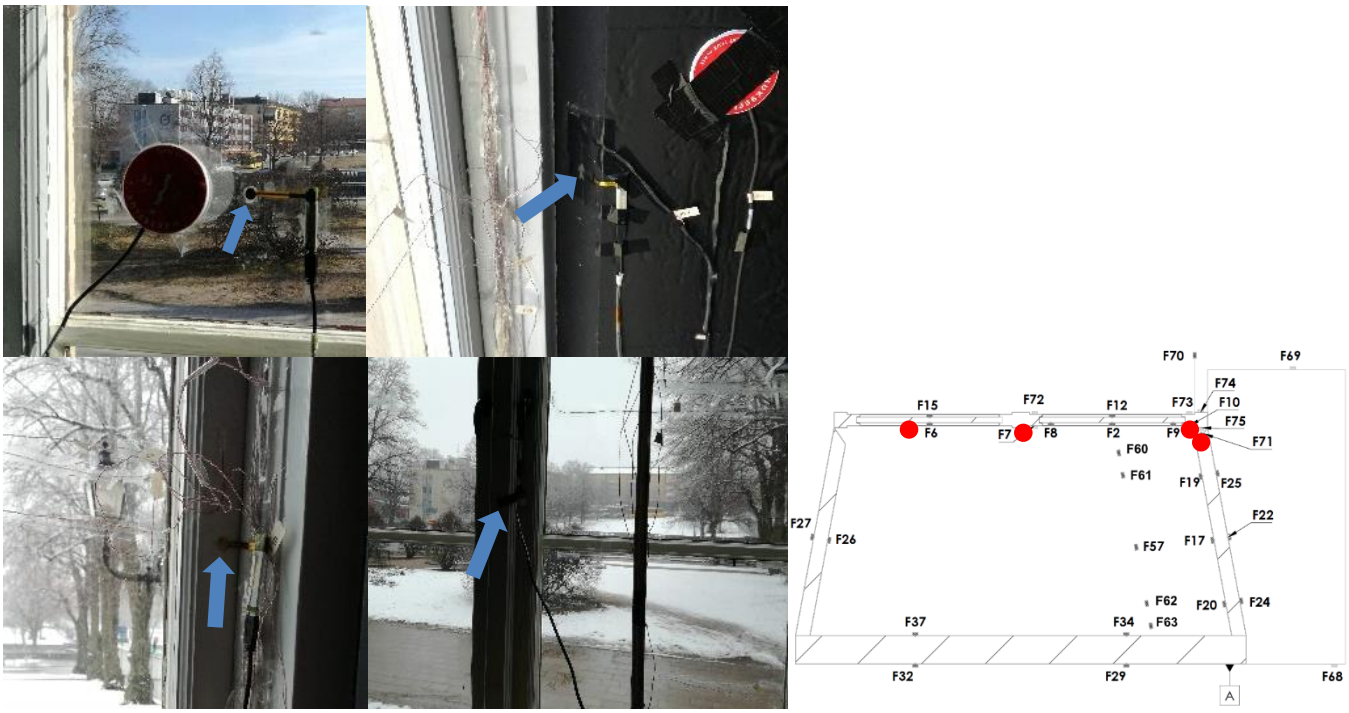

a b

FIGURE 3. 6. FIELD TEST POSITIONS OF THE SENSOR. A, CLOCKWISE FROM TOP LEFT: GLAZING, INSULATION, CENTRAL WOOD FRAME AND LATERAL WOOD FRAME. B, LOCATIONS OF THE TESTS FROM A FLOOR VIEW OF THE WINDOW.

It is meant to study the dynamics of the sensor on the different locations, check for irregularities and test its reliability. It is also possible to compare some of the measurements with the installed thermocouples and estimate the thermal conductivity of the wooden frame, for instance.

Finally, it was also planned to make tests in *Gävle Energi* facilities, on district heating network pipes. However due to lack of time and difficulties to set a date with the company it was not possible to perform those tests.

In these pipes facilities it is monitored the temperature and velocity of the liquid. The objective of that test is to determine correctly the temperature of the flowing liquid it will be used the theory explained in item 2.6. Since the installations are monitored it can be easily check if the *JonDeTech* sensor reading is correct.

3.4 Comparison with other heat flow sensors

The most used heat flux sensor in the University of *Gävle* projects is *Hukseflux* HFP01 sensor [27]. Since the faculty is very rooted to this device, it was also performed a comparison between heat flux sensor products from *JonDeTech* and *Hukseflux*.

Under the same conditions for both sensors, data acquisition was performed and the results were compared graphically and statistically:

- On field: in the *Gävle* city hall project, the comparison could be made when placed on the window glazing only. However, both sensors had different data acquisition times so a harmonizing process to merge the timestamps had to be done after the measurements took place.
- In laboratory facilities: the calibration assembly was built wide enough to fit the larger *Hukseflux* device, Figure 3. 7. It was tested under the same conditions the laboratory work took place for the *JonDeTech* sensor. As it is explained in point 3.1, both heater temperatures were set in order to create an adiabatic condition between them and the air temperature inside the climate chamber was set lower than the heaters to allow the heat to travel upwards through the device.

FIGURE 3. 7. THE TWO EXPERIMENTS THAT TOOK PLACE IN THE LABORATORY FACILITIES INVOLVING *HUKSEFLUX* SENSOR. ON THE LEFT, A TRANSIENT TEST WHERE THE BOX WAS KEPT AT 20 °C AND PUT INTO THE CLIMATE CHAMBER AT 10 °C. ON THE RIGHT THE *HUKSEFLUX* SENSOR WITHIN THE CALIBRATION ASSEMBLY.

After that, the calibration line from laboratory work was used to adjust the *JonDeTech* measurements from the city hall so that it could be checked how the previous measurements were affected by the empirical correction applied.

4 Results and discussion

Results of the thesis are exposed below on this point and discussed accordingly.

4.1 Laboratory work

Firstly, the temperature difference between the thermocouples (ΔT Calib) on the hot and the cold side (Figure 3. 2) and the sensed by the tested device (ΔT Jon) are disparate because of the conductive film position, it adds an extra layer when measuring with thermocouples. Figure 4. 1 shows this interaction. At the same time it shows that the heat transfer process is linear. However, when simulating the same situation on Comsol Multiphysics it is shown on equation 14 a similar correlation of temperatures, data is displayed on Table 4. 1, which indicates that the simulation is reliable in this part.

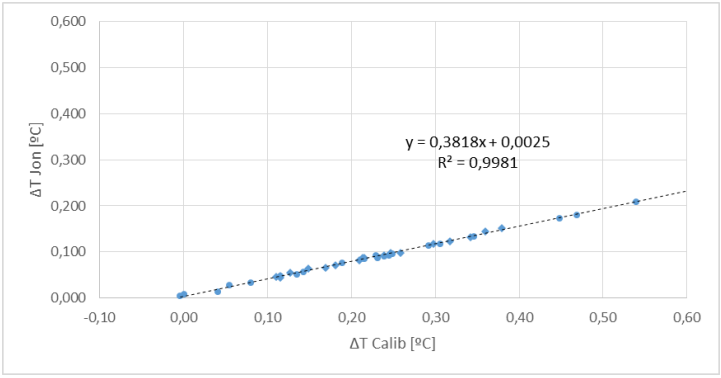

FIGURE 4. 1. CORRELATION BETWEEN THE THERMOCOUPLE MEASUREMENTS, ΔT CALIB AND *JONDETECH* SENSOR MEASUREMENTS, ΔT JON.

TABLE 4. 1. TEMPERATURES AND TEMPERATURE DIFFERENCES OF THE CALIBRATION SET UP SIMULATION.

[K]	Upper surface	Lower surface	ΔT
ΔT Jon	295.06	295.09	0.03
ΔT Calib	295.04	295.11	0.07

$$\Delta TJon = 0.428 \cdot \Delta TCalib \quad (14)$$

Secondly, calibration lines were determined for the data stored in Table 4. 2. Each variable in the table is explained below:

- Tag: Order number
- External: Temperature outside the calibration assembly set on the climate chamber
- ϕ Calib: Supplied heat
- q Calib: Heat flux on the surface inside the insulating foam
- q Calib top: Heat flux on the sensor layer, a correction extracted from the simulations was applied (explained in point 4.2.2)
- T Hot: Temperature read by the thermocouples on the warm side of the sensor
- T Cold: Temperature read by the thermocouples on the cold side of the sensor

- Δt Calib: $Thot - TCold$
- q Jon: Heat flux measurements from the tested sensor
- T Jon: Absolute temperature read by the tested sensor
- Δt Jon: Temperature difference between sensor surfaces measured by the tested sensor.

TABLE 4. 2. CALIBRATION DATA FOR *JONDETECH* SENSOR TAKEN PLACE ON THE LABORATORY.

Tag	External [º C]	ϕ Calib [W]	q Calib [W/m²]	q Calib top [W/m²]	T hot [º C]	T cold [º C]	Δt Calib [º C]	q Jon [W/m²]	T Jon [º C]	Δt Jon [º C]
1	0	0.66	119.10	101.23	2.63	2.45	0.18	95.32	-0.55	0.058
2	0	1.41	254.07	215.96	4.55	4.22	0.33	193.89	1.46	0.118
3	0	2.64	476.38	404.92	7.98	7.35	0.63	355.55	4.93	0.216
4	20	1.63	293.77	249.70				241.21		0.149
5	20	2.00	360.90	306.76	26.49	25.90	0.59	294.95	23.87	0.181
6	20	2.88	519.69	441.74	29.01	28.20	0.81	419.24	26.40	0.257
7	40	0.72	129.92	110.43	42.20	42.00	0.20	105.36	40.10	0.064
8	40	2.02	365.05	310.29	46.11	45.58	0.53	293.96	43.95	0.181
9	40	3.00	541.34	460.14	49.30	48.64	0.66	428.78	47.10	0.262
10	60	0.78	140.75	119.64	62.20	61.90	0.30	137.56	60.46	0.084
11	60	1.72	309.65	263.20	64.80	64.30	0.50	285.37	62.98	0.174
12	60	2.20	396.99	337.44	66.35	65.57	0.78	376.08	64.55	0.231

Figure 4. 2a is a scatter plot that shows the measurements versus supplied heat with the applied correction (qJon – qCalib). The regression line shows that the measurement is quite accurate even though it can be improved. However, when the data is stratified by the external set temperature in Figure 4. 2b, it can be seen a tendency of the calibration line to a higher slope.

a

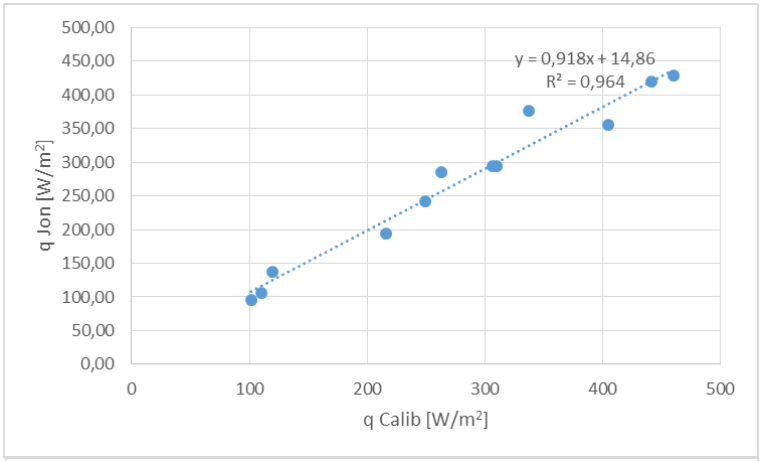

b

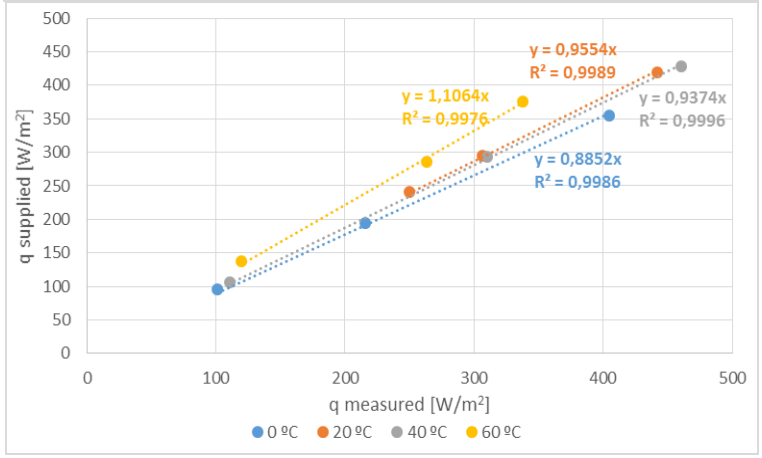

FIGURE 4. 2. SCATTER PLOT OF THE SUPPLIED HEAT FLUX AGAINST THE READINGS OF THE TESTED SENSOR. FIGURE B SHOWS THE SAME DATA BUT CLUSTERED BY THE EXTERNAL TEMPERATURE.

Next, it may be observed that variable, from Table 4. 2, TJon should be between THot and TCold interval. However, that is not the case which indicates that temperature reading is not correct, it always appear a couple of degrees lower as represented in Figure 4. 3 where red dots are the sensor readings and black lines the thermocouple intervals for the three first experiments.

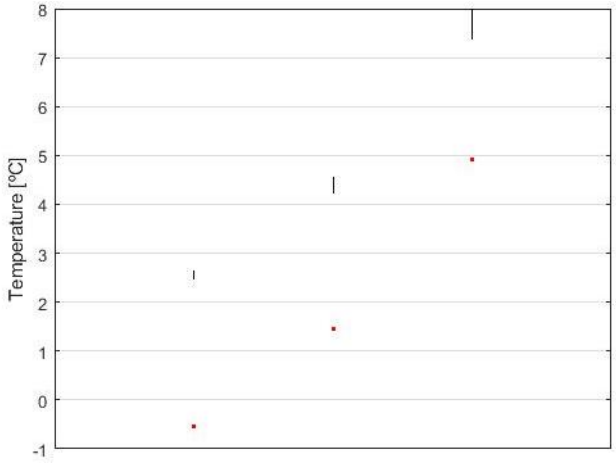

FIGURE 4. 3. BOX PLOT OF THE THREE FIRST EXPERIMENTS FROM TABLE 4.2, WHERE TJON (RED DOTS) AND THOT – TCOLD INTERVALS (BLACK LINES) ARE REPRESENTED.

Finally, if the heat flux is expressed in terms of voltage read by *JonDeTech* sensor, it can be written as equation 15 shows below.

$$q\left[{}^{W}/_{m^2}\right] = C_T(T) \cdot V[\mu V] \qquad \textbf{(15)}$$

Where coefficient C_T varies with the temperature. In the studied cases it changed within the range: $[0.166 - 0.212]$.

4.2 Computer simulations

Regarding the finite element simulations, its results and acknowledgments are exposed on the current point.

4.2.1 Simplified version of the sensor

On Figure 4. 4a it is shown a simplified version of the sensor whereas on Figure 4. 4b all the parts are included in the simulation. Both simulations differ only by 1.5 ºC while same boundary conditions are set. Moreover, the heat flux going through the sensor only differs on 1 W/m^2 (a variation from 2074 to 2075 W/m^2). At sight of the results, it is concluded that the simplification is a good approximation. Also, it reduces the meshing elements from $245{\cdot}10^3$ to $227{\cdot}10^3$ as well as the computational time from 5 hours to 30 min so, from now on the following simulations will compute the simplified version.

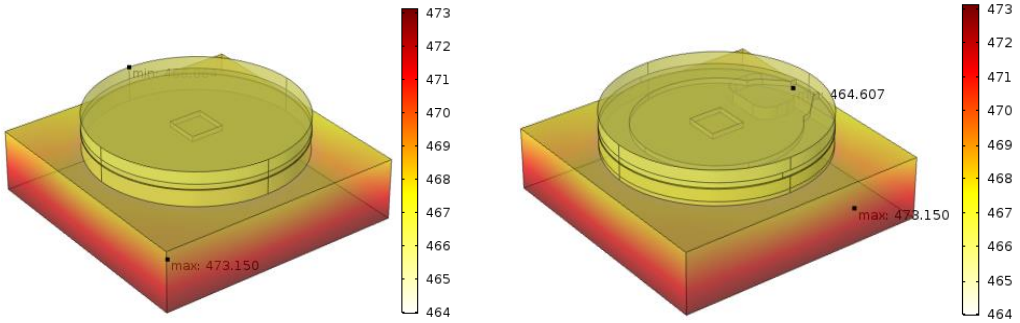

FIGURE 4. 4. SIMULATION CAPTURES OF BOTH *JONDETECH* VERSIONS. A: SIMPLIFIED VERSION, B: DETAILED VERSION.

4.2.2 Calibration assembly

The whole assembly showed in Figure 3. 2 and Figure 3. 4 was replicated in Comsol Multiphysics. Its simulation was useful to adjust the supplied heat going through the sensor and to ensure that the hypothesis taken was correct.

Firstly, it was noticed that heat was being lost through the lateral surface of the cylinder assembly, on the space between the heaters and the sensor about 5% of the heating input was spreading through the side, the values are shown on Table 4. 3.

TABLE 4. 3. HEAT FLUXES SUPPLIED AND LOST THROUGH THE DIFFERENT SURFACES OF THE ASSEMBLY.

Supplied by the heater (W/m^2)	Heat lost downwards (W/m^2)	Heat lost through lateral surface (W/m^2)
-40.81	0.06	1.97

Next, it was also noticed that thermocouples and sensor connections were helping the heat to escape from the insulation by creating a thermal bridge themselves. On Figure 4. 5 it can be observed that a thermocouple placed on the top side makes the red arrows, which represent the heat flux, bigger than on the rest of the lateral cylinder surface. About 10% of the supplied heat is being lost through sensor connections and control thermocouples.

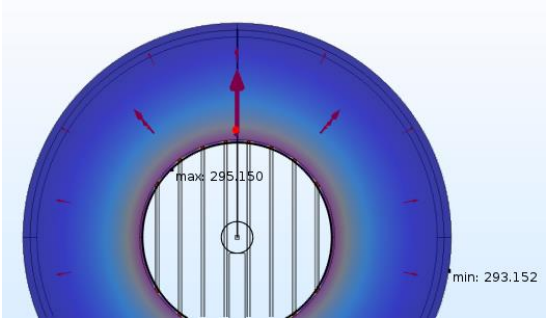

FIGURE 4. 5. TOP VIEW OF THE CALIBRATION ASSEMBLY. AT 12 O'CLOCK THERE IS A SIMULATED THERMOCOUPLE WIRE. RED ARROWS ARE PROPORTIONAL TO HEAT FLUX, IT CAN BE SEEN THAT THEY GROW BIGGER THE CLOSER TO THE WIRE.

After that it was checked that the heat flux arriving to the sensor was uniform and normal to its surface, as showed on Figure 4. 6.

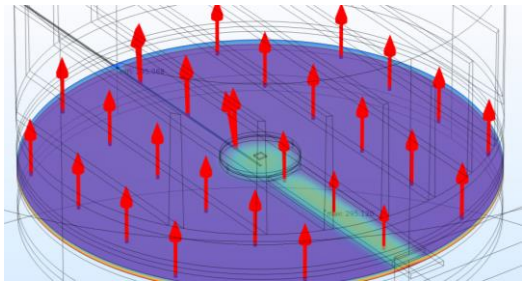

FIGURE 4. 6. HEAT FLUX JUST BEFORE HITTING THE SENSOR. IT IS OBSERVED THAT ALL THE ARROWS ARE THE SAME LENGTH AND POINTING UPWARDS (NORMAL TO SENSOR SURFACE).

4.2.3 Sensor under the influence of convection

Next study replicated a part of the window glazing with the sensor stuck on it. Results are shown on Figure 4. 7. The back ground gradient represents the velocity of the flowing air and the black lines next to the sensor represent the trace of an air particle. At sight of the results, it can be observed that the sensor remains inside the boundary layer of the air near the glass.

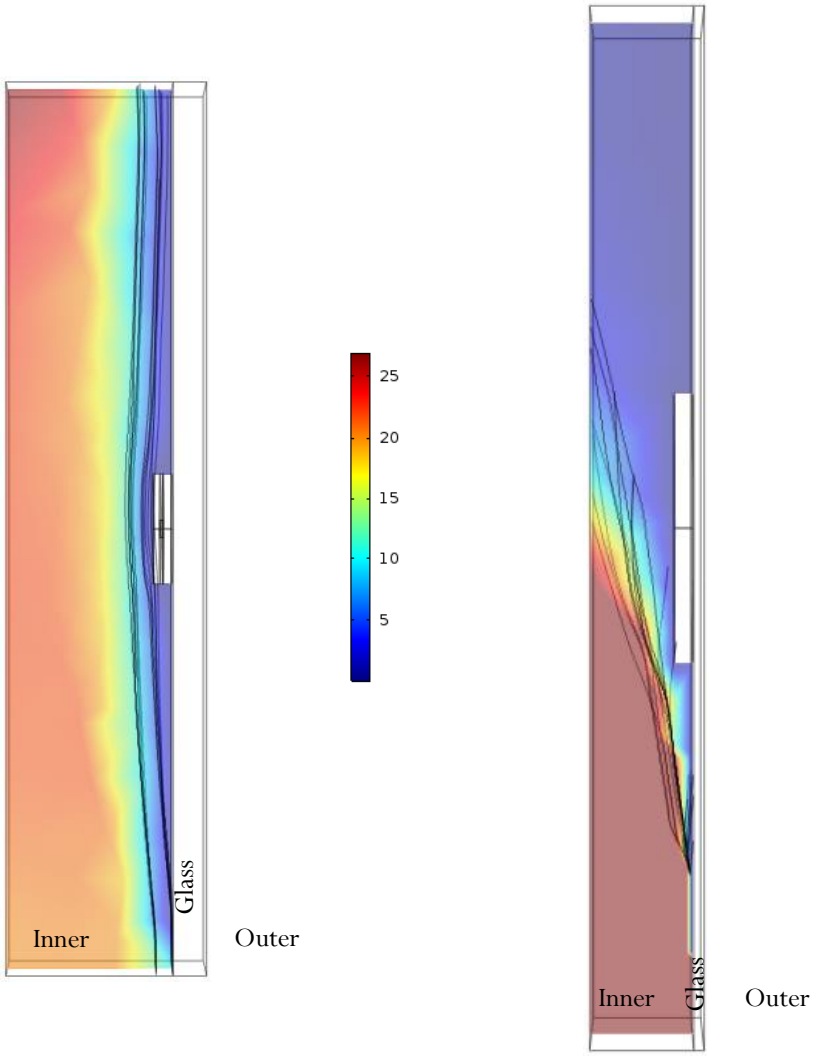

FIGURE 4. 7. LEFT: VELOCITY AND TRACE RESULTS OF *JONDETECH* ON A GLASS AND AIR FLOW SIMULATION.
FIGURE 4. 8. RIGHT: VELOCITY AND TRACE RESULTS OF *HUKSEFLUX* ON A GLASS AND AIR FLOW SIMULATION.

After that it was simulated the same scenario with *Hukseflux* sensor, which is thicker. As seen on Figure 4. 8, for this other sensor the particle's traces (black lines) are a lot more turbulent so, this indicates that the boundary layer is being altered by the presence of the device.

Lastly, it was also compared the situation of the sensor on the laboratory calibration assembly and on the glass at field measurements. Figure 4. 9 shows the difference of behaviour: on the glass (a) the heat flux has a no-normal direction because it is subjected to flowing air, the heat seems to be spreading through the brass encapsulating and avoiding the kapton sensing part that is located on the very centre of the device, which may cause inaccurate measurements; on the calibration assembly (b) the heat spreads a little through the sensor but the combined total appears to be normal to the surface. This finding could suggest two points:

- A metal encapsulation is not the best material to build this thermal sensor since it causes the heat to be conducted away from the sensing part.
- Calibration lines determined in the laboratory may not be accurate to the reality on the glazing because of the heat flux direction difference on both situations.

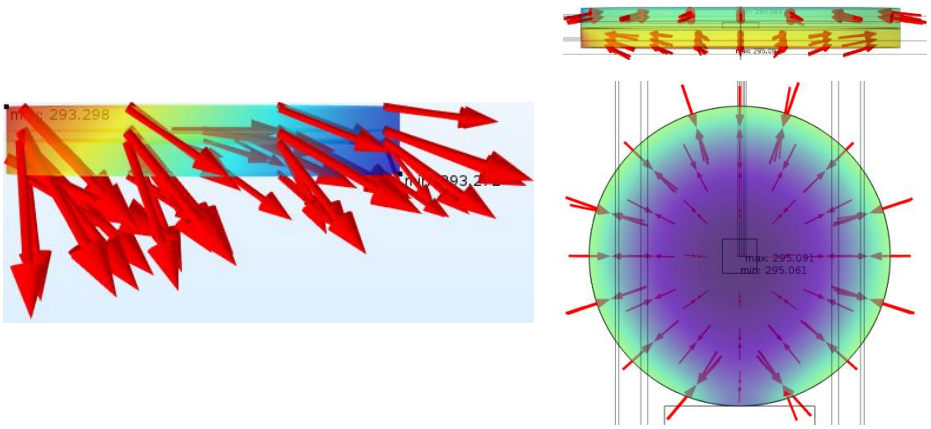

a b

FIGURE 4. 9. A: HEAT FLUX ARROW PLOT ON THE WINDOW GLAZING. B: ELEVATION AND FLOOR OF HEAT FLUX ARROW PLOT ON THE CALIBRATION ASSEMBLY.

4.3 Field measurements

Last part of the method consisted in making measurements outside the laboratory facilities in *Gävle* city hall windows and on pipes. However, at the end it was not possible to make measurements on water pipes unfortunately.

These first results are obtained with the sensor inbuilt calibration data, later adjustments are applied in point 4.4 based on Comsol simulation results.

Still, measurements from the city hall indicate that the dynamics of the thermopile are correct and quite accurate if a look is taken at Figure 4. 10, a time series of the data acquisition when placing both sensors on the window glazing. It may be observed that even though the values of qJon are a bit higher than qHF they follow the same dynamics. This dissimilarity may be caused by the fact that both devices are sensing different heat fluxes (one remains inside the boundary layer while the other one disturbs it and therefore senses outside it). However, *Hukseflux* would measure larger heat fluxes than *JonDeTech*, since it "shortcuts" the boundary layer.

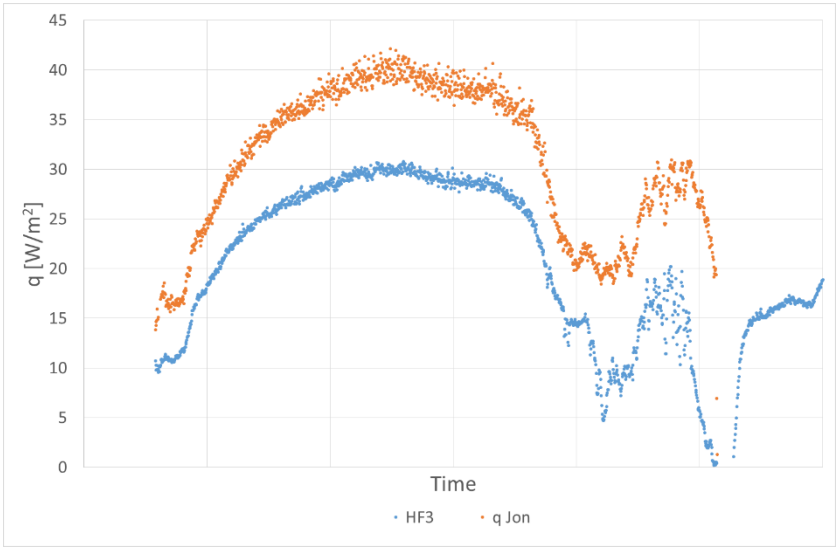

FIGURE 4. 10. TIME SERIES OF THE GLAZING ORANGE QJON IS THE READING FROM THE TESTED SENSOR AND QHF IS THE READING FROM ONE OF THE USED *HUKSEFLUX* SENSOR BY THE COLLEGE.

Finally, the remaining measurements from the city hall cannot be compared with other measurement sources but, all the results make sense and its dynamics are consistent with the various spots where the sensor was placed, see Figure 4. 11.

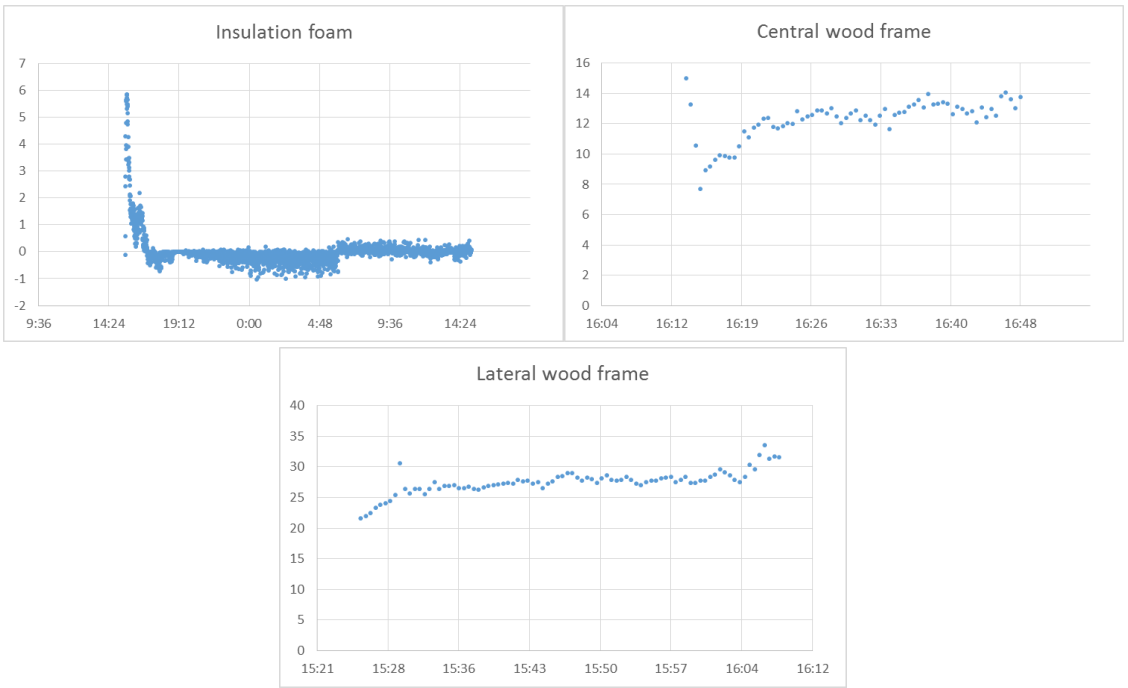

FIGURE 4. 11. RESULTS FOR THE STUDIED SENSOR ON THE DIFFERENT LOCATIONS OF FIELD MEASUREMENTS.

In the case of the lateral wooden frame, it is possible to use the measurements from two thermocouples one outside and one inside surfaces to calculate an approximate thermal conductivity for the wood. Its calculations are shown on equation 16, where $\mathbf{T_{in}}$ is the inner wood temperature, $\mathbf{T_{out}}$ is the outer wood temperature, **e** is the thickness of the frame and $\boldsymbol{\lambda}$ is the thermal conductivity for this wood.

$$q = \frac{T_{in} - T_{out}}{e/\lambda}$$

$$27 = \frac{17.7-3.7}{32[mm]/\lambda} \qquad \lambda = 0.123 \left[\frac{W}{m \cdot K}\right] \tag{16}$$

Common values for $\boldsymbol{\lambda}$ for wood are between 0.06 and $0.18\left[\frac{W}{m \cdot K}\right]$. Therefore, the obtained value is rather acceptable.

4.4 Comparison with other heat flow sensors

The measures from both sensors from Figure 4. 10 are compared against each other in a scatter plot as seen in Figure 4. 12, it can be seen a similar behaviour but not on low readings. Values contained within the red circle seems to be measured much higher than the others. It appears to be a problem with the *JonDeTech* sensor for readings lower than 10 W/m^2 approximately.

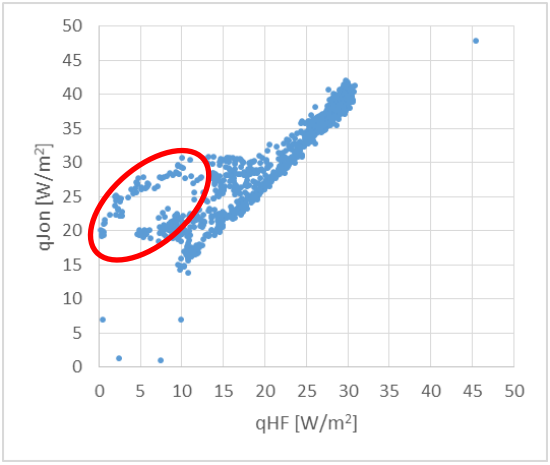

FIGURE 4. 12. SCATTER PLOT OF HEAT FLUX MEASUREMENTS FOR BOTH ANALYSED SENSORS.

After that, the data was adjusted from the field measurements with the calibration line determined by the lab. As seen in Figure 4. 13, the grey plot representing the adjusted data does not merge with the measurements from the other sensor. However, since the conditions from the lab and the field differ, it cannot be ensured that its reading is more reliable than *Hukseflux* one. Neither is true that *Hukseflux* measurements are 100 % accurate.

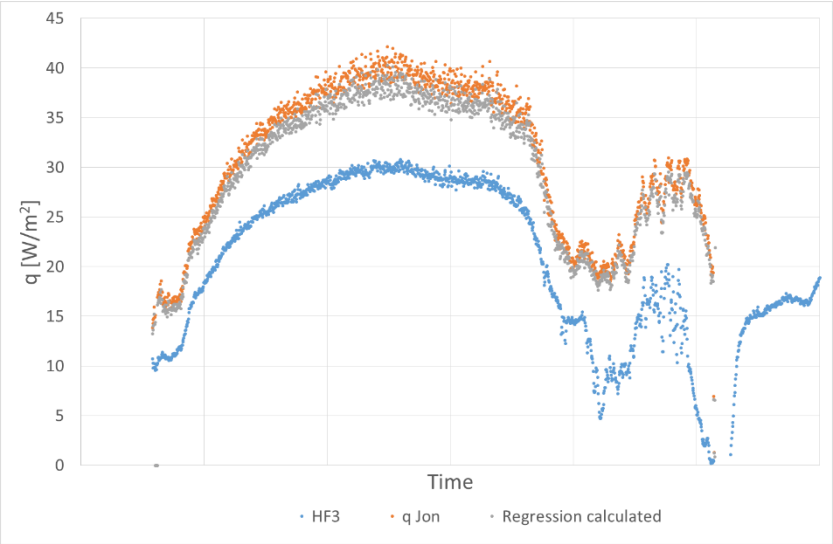

FIGURE 4. 13. SAME TIME SERIES AS FIGURE 4.10 WITH THE ADDITION OF THE CORRECTED REGRESSION LINE DETERMINED BY THE LABORATORY TESTS.

On the other hand, tests in the calibration assembly were redone with *Hukseflux* sensor. The results compared with the previous ones are plotted on Figure 4. 14, here it can be observed that qHF, which is the measurement for *Hukseflux*, adjusts almost perfectly with the supplied heat with a tilt of 0.9805. It is also worth of mention that there is no temperature dependency on this sensor, same temperature modifying conditions were applied but there was no reason to cluster the data.

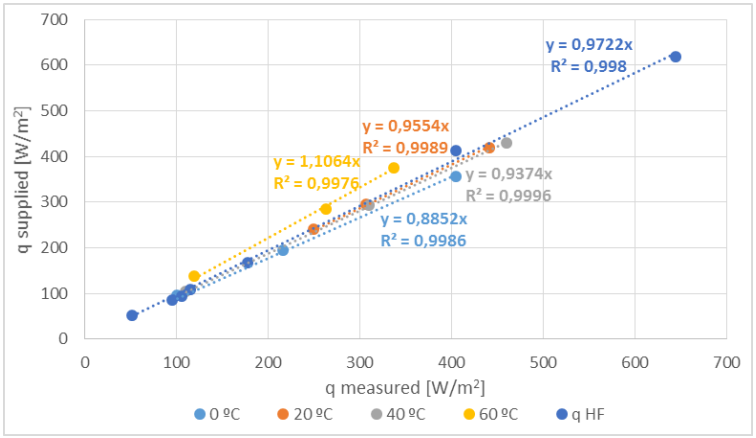

FIGURE 4. 14. SCATTER PLOT OF SUPPLIED HEAT AGAINST SENSORS MEASUREMENTS.

4.5 Method discussion

The applied method combined computer simulations, field arbitrary measurements and laboratory controlled measurements. By using different methods it was intended to use more than one approach to the problem and this mixture of methods allowed to apply corrections when they were needed, so that the accuracy of the previous experiments could be improved.

Nevertheless, at the sight of the results from the computer simulations, some aspects could be redesigned in order to improve the experiments performance. That is:

- To place fewer thermocouples inside the calibration assembly will reduce heat losses through the wiring which are currently 10% of the supplied to the heaters.
- To monitor natural heat variables in the field measurements. By placing the sensor next to another reading device more sources of comparison will be available so that the results could be check against the studied sensor.
- In order to determine the temperature dependency, the boundary temperature conditions can be better modified and analysed. It could be also used the temperature read by the sensor and not the external set on the climate chamber, with that the accuracy of the calibration lines will be improved as well.

5 Conclusions

5.1 Study results

Here, the findings of the thesis regarding the testing and calibration of *JonDeTech* heat flux sensor are explained.

Firstly, it was determined four calibration lines for different temperature conditions, as are expressed in Figure 4. 2b. It can be observed a slight temperature dependency. It was also noticed that temperature measurement from *JonDeTech* sensor always reads about 1.5 °C lower than the real temperature.

Secondly, looking at the calibration assembly, a correction of the supplied heat was applied because it was being lost about 15% of it through the insulation and the installed wires. It was also confirmed that the calibration heat flux though the sensor was uniform and normal to its surface.

Compared with the other sensor, *JonDeTech* sensor does not disturb the air boundary layer near the surface where it is placed whereas the other one does. Therefore, it can be deduced that both sensors are not measuring under same conditions. However, a metal encapsulation may not be the best material to build *JonDeTech* thermal sensor since it causes the heat to be conducted away from the sensing part or actually the non-uniform heat transfer is increasing the heat flow through the sensor, since the sensor indicates a higher value in comparison to the market sensor (*Hukseflux*). Also, it is important to notice that calibration lines determined on the laboratory may not be accurate to the reality on the glazing because of the heat flux direction difference on lab scenario and in field scenario.

On the other hand, the dynamics observed on the field measurements are as they would be expected for each case. Even though it was not possible to verify the values due to the impossibility to monitor accurately natural variables.

Finally, regarding the comparison with other sensors, some small measurement deviations were noticed. However, it was not possible to conclude which reading is more reliable. Last, at low heat flux values *JonDeTech* sensor measurements seem to behave poorly, the difference with the other sensor is accentuated when it comes to values lower than 10 W/m^2.

5.2 Outlook

Upcoming work should be focused in solving the difference of the heat flux direction between tests in laboratory facilities and on field as well as the problem with the heat conducted away through the brass encapsulation.

The first issue could be studied by testing in laboratory environment the sensor and applying a heat flux not normal to the surface resembling in some manner the field measurements. It is related to the second issue as well, since a better guard may cause the incidental heat flux to be received normally to the surface. Therefore, each improvement on the first issue should be retested on the second one and vice versa.

Regarding the encapsulation issue, it could be analysed by trying different guard materials, such as ceramics or plastics. Of course, taking into account that it should have a similar thermal conductivity as the sensor itself to prevent the reading to be higher or lower. When changing the encapsulation, another possible outcome could be to design more than one type of sensor, so that each different type will be meant to be placed over different types of surfaces, that is, for instance, one sensor designed specifically for metal surfaces, one for plastics and organic surfaces and another one for ceramic surfaces. These different sensor types would have their thermal conductivity material guards accordingly to the surfaces they will be placed over.

Not as significant from the energy systems point of view but also worth of mention, is the search of potential markets for this kind of sensors. They can have a bright future in measuring local heat flux through building and installation components. It can be interesting as well to see these sensors in other practical applications such as mobile IR temperature sensors on smartphones (which *JonDeTech* has already been working on), smart clothing that keep the wearing person warm by heating the garment, presence detectors to heat a room or turn on the lights, bioengineering sensors inside living beings, underwater applications can be also performed if the design is adjusted accordingly and a large etcetera list.

5.3 Perspectives

The current thesis can be linked to some of the seventeen global goals that the world leaders agreed to accomplish for a better world by 2030. The objectives are focused on ending the poverty, stopping climate change and fighting inequality among other purposes. They are meant to inspire governments, businesses and the general public to work as a whole and stand up to build a better world for everyone.

This thesis can help to some of the goals because of its scientific and engineering character. For instance, number seventh "Affordable and clean energy", renewable energy solutions are becoming cheaper, more reliable and more efficient every day. World's current reliance on fossil fuels is unsustainable and harmful to the planet, which is the reason why the way energy is produced and consumed needs to change. The studied sensor and the current thesis can be used to improve the thermal performance of many devices and buildings which can be classified as energy efficiency and energy saving that are a big part of clean energy.

Very close to the last point can be included number eleventh "Sustainable cities and communities", the world's population is constantly increasing. To accommodate everyone, it is needed to build modern, sustainable cities. For everyone to survive and prosper, they will be needed new, intelligent urban planning that creates safe, affordable and resilient cities with green living conditions. The studied sensor can also be used in applications that aim to verify that any system is working properly as well as to detect possible failures; qualities that will be very searched in these new intelligent cities.

It is also important to emphasise its potential in the modern day society process of digitalization, a tiny temperature sensor as the studied have and will have a large amount of technical applications. Therefore, goal number ninth "Industry, innovation and

infrastructure", which aims to create a functioning and resilient infrastructure to be the foundation of every successful community by meeting future challenges and upgrading the current infrastructures and industries, is on point as well. This will bring prosperity, create jobs and make sure that stable and prosperous societies across the globe are built.

Lastly, in a smaller scale, this thesis worked in a partnership between entities for the pursuit of a common goal. A business company, *JonDeTech AB,* and a public institution, University of *Gävle* collaborated in making this thesis possible the same way the global goals propose to work along others in their last goal; number seventeenth "Partnerships for the goals".

References

[1] M.Y. Efremov, E.A. Olson, M. Zhang, F. Schiettekatte, Z. Zhang, L.H. Allen, Ultra-sensitive, fast, thin-film differential scanning calorimeter, Review of Scientific Instruments 75 (2004) 179.

[2] J. Lerchner, A. Wolf, G. Wolf, V. Baier, E. Kessler, M. Nietzsch, M. Krügel, A new micro-fluid chip calorimeter for biochemical applications, Thermochimica Acta 445 (2006) 144-150.

[3] L. Wang, B. Wang, Q. Lin, Demonstration of MEMS-based differential scanning calorimetry for determining thermodynamic properties of biomolecules, Elsevier, Sensors and Actuators B: Chemical 134 (2008) 953-958.

[4] R. Buchner, C. Sosna, M. Maiwald, W. Benecke, W. Lang, A high-temperature thermopile fabrication process for thermal flow sensors, Elsevier, Sensors and Actuators A 130–131 (2006) 262-266.

[5] K. Keränen, J. Mäkinen, P. Korhonen, E. Juntunen, V. Heikkinen, J. Mäkelä, Infrared temperature sensor system for mobile devices, Elsevier, Sensors and Actuators A 158 (2010) 161–167.

[6] S. Thapa, S. Tangutooru, Eric J. Guilbeau, Niel D. Crews, The thermopile: An anisotropic temperature sensor, Elsevier, Sensors and Actuators A 187 (2012) 132-140.

[7] D. Bakonyi *, G. Dobszay, Simulation aided optimization of a historic window's refurbishment, Elsevier, Energy and Buildings 126 (2016) 51-69.

[8] R. Walker, S. Pavía, Thermal performance of a selection of insulation materials suitable for historic buildings, Elsevier, Building and Environment 94 (2015) 155-165.

[9] David Farmer, Chris Gorse, William Swan, Richard Fitton, Matthew Brooke-Peat, Dominic Miles-Shenton, David Johnston, Measuring thermal performance in steady-state conditions at each stage of a full fabric retrofit to a solid wall dwelling, Elsevier, Energy and Buildings 156 (2017) 404-414.

[10] J.H. Klems, Measurement of fenestration net energy performance: considerations leading to development of the Mobile Window Thermal Test (MoWiTT) facility, https://escholarship.org/uc/item/6kp503mf, 1984.

[11] Giorgio Baldinelli, Francesco Bianchi, A. Lechowska, A. Schnotale, Dynamic thermal properties of building components: Hot box experimental assessment under different solicitations, Elsevier, Energy & Buildings 168 (2018) 1-8.

[12] C. Buratti, E. Belloni, L. Lunghi, A. Borri, G. Castori, M. Corradi, Mechanical characterization and thermal conductivity measurements using of a new 'small hot-box' apparatus: innovative insulating reinforced coatings analysis, Elsevier, Journal of Building Engineering 7 (2016) 63–70.

[13] K. Martina, A. Campos-Celador, C. Escuderoa, I. Gómez, J.M. Sala, Analysis of a thermal bridge in a guarded hot box testing facility, Elsevier, Energy and Buildings 50 (2012) 139–149.

[14] Joana Prata, Nuno Simões, António Tadeua, Heat transfer measurements of a linear thermal bridge in a wooden building corner, Elsevier, Energy and Buildings 158 (2018) 194–208.

[15] Amrita Ghosh, Supratik Ghosh, Subhasis Neogi, Performance Evaluation of a Guarded Hot Box U-value Measurement Facility under Different Software Based Temperature Control Strategies, Elsevier, Energy Procedia 54 (2014) 448–454.

[16] F. Asdrubali, G. Baldinelli, Thermal transmittance measurements with the hot box method: Calibration, experimental procedures, and uncertainty analyses of three different approaches, Elsevier, Energy and Buildings 43 (2011) 1618–1626.

[17] Antonio Piccolo, Concettina Marino, Antonino Nucara, Matilde Pietrafesa, Energy performance of an electrochromic switchable glazing: Experimental and computational assessments, Elsevier, Energy & Buildings 165 (2018) 390–398.

[18] Thibault Pfluga, Nikolaus Nestle, Tilmann E. Kuhna, Monica Siroux, Christoph Maurer, Modeling of facade elements with switchable U-value, Energy & Buildings 164 (2018) 1–13.

[19] Robert Hart, Numerical and experimental validation for the thermal transmittance of windows with cellular shades, Energy & Buildings 166 (2018) 358–371.

[20] Manual on the Use of Thermocouples in Temperature Measurement (4th Ed.). 1993, 48 - 51, ISBN 978-0-8031-1466-1

[21] Ørsted, Hans C. (1823), "New experiments by Dr. Seebeck on electromagnetic effects", Annales de chimie et de physique Vol. 22, 199–201.

[22] Alan S. Morris, Reza Langari, Measurement and Instrumentation (Second Edition), 2016, 407-46, ISBN: 978-0-12-800884-3.

[23] Thermoelectric Energy Conversion: Basic Concepts and Device Applications. Hoboken, NJ: John Wiley & Sons, 67 – 76, ISBN 9783527698134.

[24] *JonDeTech AB* home page: https://www.jondetech.se/technology/ . (May 2019)

[25] *Máquinas térmicas motoras* (First edition), 99 - 106, ISBN 84-8301-644-3.

[26] D. Prakash, P. Ravikumar, Analysis of thermal comfort and indoor air flow characteristics for a residential building room under generalized window opening position at the adjacent walls, Elsevier, International Journal of Sustainable Built Environment (2015) 4, 42-57.

[27] *Hukseflux AB* home page: https://www.hukseflux.com/products/heat-flux-sensors/heat-flux-meters/hfp01-heat-flux-sensor . (May 2019)

Appendix A

In this appendix a detailed drawing for each part of the calibration device/assembly is presented. It can be found on next page.

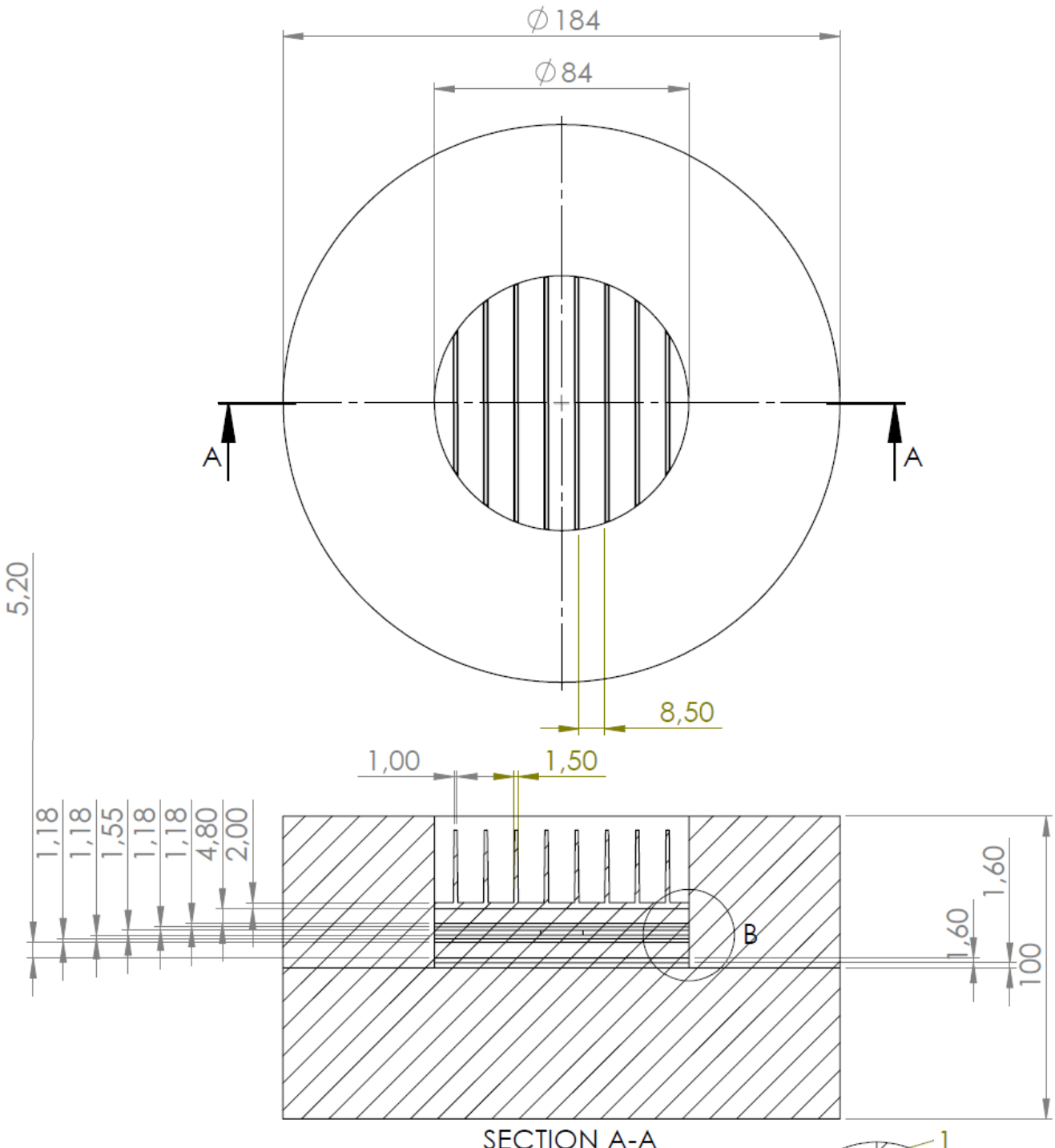

SECTION A-A

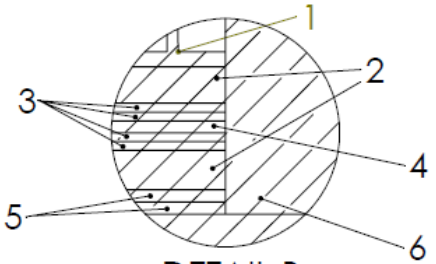

DETAIL B
SCALE 1 : 1

ID	Material
1	Aluminium fins and base
2	Copper
3	Conductive film with thermocouples
4	Brass
5	FR4 proboard with heaters on top
6	Insulation Kingspan

Name:
Calibration device

Drawing num:
001

Autor:
Hector Sanchez

A4

SCALE 1:2

SHIT 1 / 1